# Supporting Information

Zandarashvili et al. 10.1073/pnas.1121500109

## SI Methods.

**Residual Dipolar Coupling (RDC) Prediction of $^1D_{NH}$ from Molecular Shape and Charge Distribution for the Specific Complex.** $^1D_{NH}$ couplings for the specific complex of Egr-1 with 28-bp DNA SP28 were predicted from the shape and charge distribution by using the program PALES (1, 2). For this calculation, a structure of the specific complex with DNA SP28 (Fig. S1*A*) was built from the 1.6-Å resolution crystal structure of the specific complex with 12-bp DNA (PDB 1AAY) by extending B-form DNA structures with the XPLOR-NIH software (3, 4).

**RDC Prediction of $^1D_{NH}$ from Molecular Shape and Charge Distribution for the Nonspecific Complex (No Domain Motions).** RDC $^1D_{NH}$ data for the nonspecific complex were predicted for a case in which the three zinc finger domains of Egr-1 bind to a nonspecific site in the same mode as seen for the crystal structure of the specific complex with a target DNA. Structure models for nonspecific 28-bp DNA complexes of Egr-1 at 18 different binding sites (Fig. S1*B*) were generated from the crystal structure of the specific complex (PDB 1AAY) by extending B-form DNA. The other 18 states with the opposite protein orientation can also be represented with these 18 structures (e.g., the opposite orientation at the binding site of model 1 corresponds to model 18). It should be noted that base sequence is not an important factor for the RDC prediction based on the overall molecular shape and charge distribution. For each structure, the alignment tensor and RDCs were predicted with PALES on the basis of the 3D shapes and charge distributions.

**RDC Prediction of $^1D_{NH}$ from Molecular Shape and Charge Distribution for the Nonspecific Complex (with ZF1's Domain Motions).** RDC $^1D_{NH}$ data for the nonspecific complex were also predicted for a case where ZF1 undergoes substantial domain motions while ZF2 and ZF3 bind a nonspecific site in the same mode as seen for the crystal structure of the specific complex with a target DNA. For this consideration, we generated a structure ensemble with ZF1's position altered by a high-temperature rigid-body dynamics calculation in a torsion angle space using XPLOR-NIH. In the dynamics calculations, ZF1's backbone was treated as a rigid body and could undergo collective motions due to conformational freedoms given to Linker 1 while the atomic coordinates of DNA and ZF2 and ZF3 were kept fixed during the calculation. The bond, angle, improper, and van der Waals energy terms as well as the conformational database pseudoenergy term (5–7) were used for keeping reasonable conformations. Initially, the rigid-body dynamics calculation was performed at 5,000 K for a 30-ps period starting with the crystal structure of the specific complex of Egr-1, and then the temperature was gradually reduced from 5,000 K to 25 K through 60 cycles of 1.2-ps periods. Fifty structures with ZF1 positioned differently in the complex were obtained. Using these structures, 18 ensembles of 28-bp nonspecific complexes of Egr-1 at different sites (Fig. S1*C*) were generated (the total number of structures, 900[$= 50 \times 18$]). For each of them, the alignment tensor and RDC $^1D_{NH}$ couplings were predicted from molecular shape and charge distribution by using PALES.

**Estimation of the Timescale of ZF1's Domain Motions in the Nonspecific DNA Complex of Egr-1.** As described in the main text, $^{15}N$ $R_2$ data for the nonspecific complex are highly influenced by protein translocation on DNA that occurs on a μs–ms timescale. This makes quantitative analysis of fast domain dynamics nontrivial. Here, we estimated the timescale of ZF1's domain motions in the nonspecific complex from $^{15}N$ $R_1$ and heteronuclear NOE data alone. The analysis made use of the spectral density function of the extended model-free approach (8, 9):

$$J(\omega) = \frac{2}{5}\left\{\frac{S_f^2 S_s^2 \tau_r}{1+\omega^2\tau_r^2} + \frac{(1-S_f^2)\tau_1}{1+\omega^2\tau_1^2} + \frac{S_f^2(1-S_s^2)\tau_2}{1+\omega^2\tau_2^2}\right\} \qquad [S1]$$

where $\tau_r$ represents the correlation time for molecular tumbling; $S_s^2$, $S_f^2$,$\tau_s$, and $\tau_f$, order parameters and correlation times for slow and fast internal motions; $\tau_1 = (\tau_c^{-1} + \tau_f^{-1})^{-1}$; and $\tau_2 = (\tau_c^{-1} + \tau_s^{-1})^{-1}$. Here, the fast motions correspond to internal motions of N-H bond vectors within the framework of ZF1; whereas, the slow motions correspond to ZF1's domain motions in the molecular framework of the nonspecific complex. From the $^{15}N$ $R_1$, $R_2$, and heteronuclear NOE data, we determined the order parameters and correlation times for N-H bond vectors in the specific complex (Fig. S2*A*). Based on the order parameters and correlation times for the specific complex, along with the two assumptions given in the main text, we estimated $S_s^2$ and $\tau_s$ for ZF1's domain motions in the nonspecific complex via minimization of:

$$\chi^2 = \frac{(R_{1,600}^{obs} - R_{1,600}^{cal})^2}{\sigma_{R1,600}^2} + \frac{(R_{1,800}^{obs} - R_{1,800}^{cal})^2}{\sigma_{R1,800}^2} + \frac{(NOE_{600}^{obs} - NOE_{600}^{cal})^2}{\sigma_{NOE,600}^2} + \frac{(NOE_{800}^{obs} - NOE_{800}^{cal})^2}{\sigma_{NOE,800}^2} \qquad [S2]$$

in which observed and calculated quantities are denoted by obs and cal, respectively; and, $\sigma$ represents experimental uncertainty. The calculations were carried out for the secondary structure regions of ZF1 (Fig. S2*B*).


1. Zweckstetter M (2008) NMR: Prediction of molecular alignment from structure using the PALES software. *Nat Protoc* 3:679–690.
2. Zweckstetter M, Hummer G, Bax A (2004) Prediction of charge-induced molecular alignment of biomolecules dissolved in dilute liquid-crystalline phases. *Biophys J* 86:3444–3460.
3. Schwieters CD, Kuszewski JJ, Clore GM (2006) Using Xplor-NIH for NMR molecular structure determination. *Prog Nucl Mag Res Sp* 48:47–62.
4. Schwieters CD, Kuszewski JJ, Tjandra N, Clore GM (2003) The Xplor-NIH NMR molecular structure determination package. *J Magn Reson* 160:65–73.
5. Clore GM, Kuszewski J (2002) $\chi_1$ Rotamer populations and angles of mobile surface side chains are accurately predicted by a torsion angle database potential of mean force. *J Am Chem Soc* 124:2866–2867.
6. Kuszewski J, Gronenborn AM, Clore GM (1996) Improving the quality of NMR and crystallographic protein structures by means of a conformational database potential derived from structure databases. *Protein Sci* 5:1067–1080.
7. Kuszewski J, Gronenborn AM, Clore GM (1997) Improvements and extensions in the conformational database potential for the refinement of NMR and X-ray structures of proteins and nucleic acids. *J Magn Reson* 125:171–177.
8. Baber JL, Szabo A, Tjandra N (2001) Analysis of slow interdomain motion of macromolecules using NMR relaxation data. *J Am Chem Soc* 123:3953–3959.
9. Clore GM, et al. (1990) Deviations from the simple 2-parameter model-free approach to the interpretation of N-15 nuclear magnetic-relaxation of proteins. *J Am Chem Soc* 112:4989–4991.

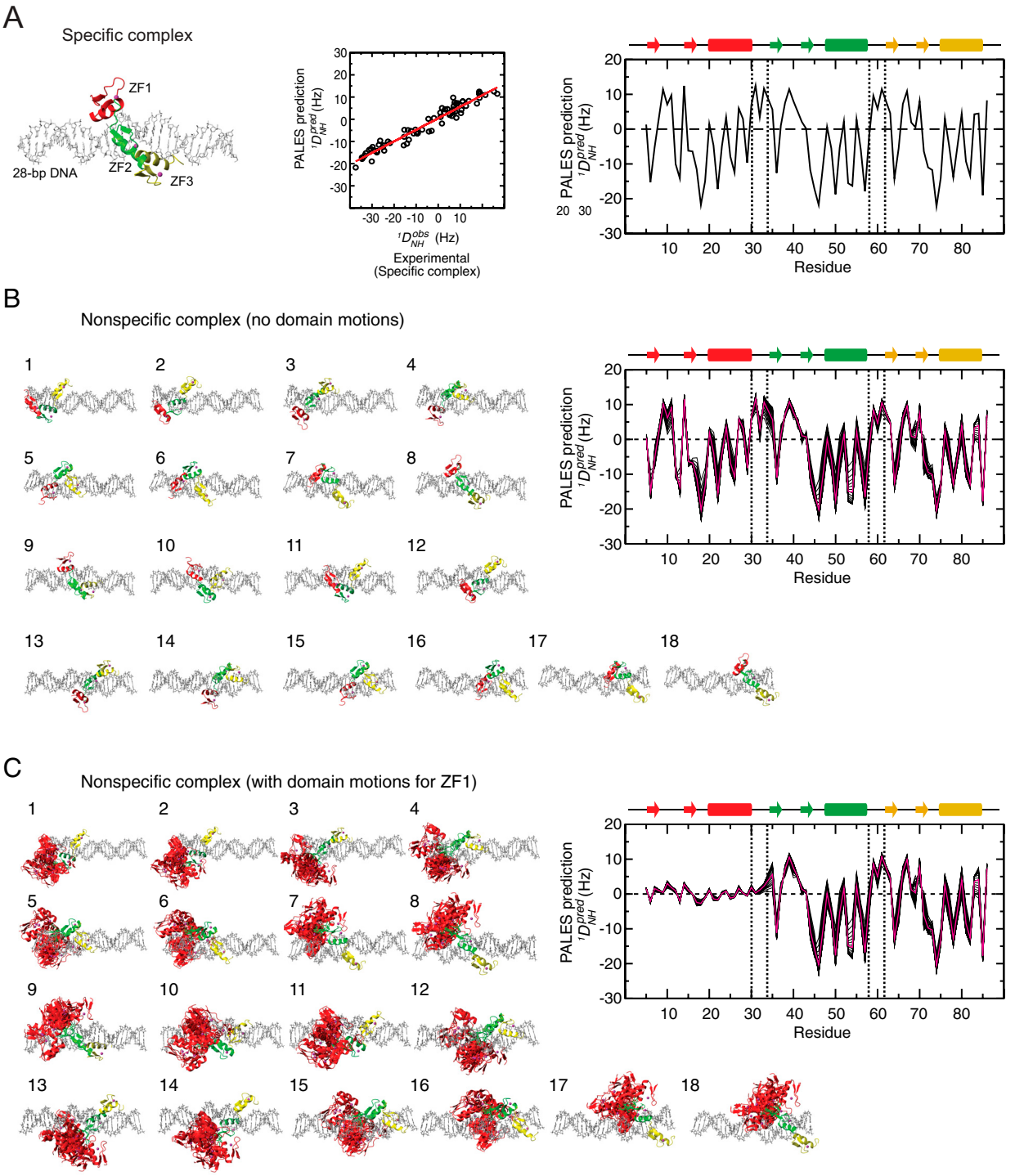


**Fig. S1.** Prediction of Pf-1-induced RDC $^1D_{NH}$ data by using the program PALES based on molecular shape and charge distribution. (*A*) Prediction for the specific complex of Egr-1 with 28-bp DNA. Predicted RDC $^1D_{NH}$ for individual residues of Egr-1 as well as the correlation between the predicted and experimental RDC $^1D_{NH}$ for the specific complex are shown. Despite the absence of any parameter optimization, the correlation was excellent, presumably because relatively strong electrostatic effects of 28-bp DNA on molecular alignment of the complex can be calculated accurately. (*B*) Prediction for the nonspecific complex of Egr-1 under the assumption that all the three zinc finger domains binds to each DNA site in the same way as seen in the crystal structure of the specific complex. Structure models for the nonspecific 28-bp DNA complex of Egr-1 at 18 different sites were used. RDC $^1D_{NH}$ for individual residues for each model are shown. Because negative charges of DNA govern the electrostatically driven alignment of the complex, the profiles of predicted RDCs are similar regardless of the protein's position. Ensemble averages of RDC $^1D_{NH}$ for the 18 models are shown in magenta. (*C*) Prediction for the nonspecific complex under the assumption that ZF1 undergoes domain motions while ZF2 and ZF3 of Egr-1 binds to each DNA site in the same way as seen in the crystal structure of the specific complex. The shown structure ensembles for the nonspecific 28-bp DNA complex of Egr-1 at 18 different sites were used for the calculation. ZF1's domain motions are represented by 50 different structures obtained by high-temperature, rigid-body dynamics calculations (*SI Text*). RDC $^1D_{NH}$ for individual residues of Egr-1 at 18 different sites are shown together with averages of RDC $^1D_{NH}$ for the 18 ensembles (magenta). Details of these calculations are given in *SI Methods*.

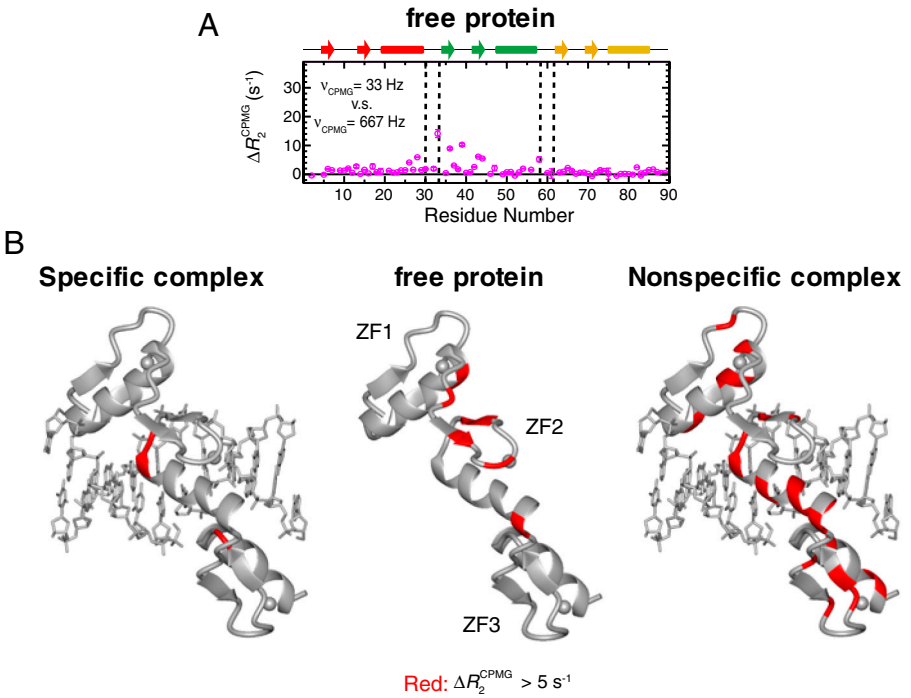


**Fig. S2.** Comparison of μs-ms dynamics as detected by $^{15}$N CPMG experiments for the free protein, the nonspecific complex, and the specific complex. (*A*) Differences between apparent $R_2$ rates at CPMG frequencies $\nu_{CPMG}$ of 33 Hz and 667 Hz [$\Delta R_2^{CPMG} = R_2(33\ Hz) - R_2(667\ Hz)$] for the free Egr-1 protein. The data were collected at a $^1$H frequency of 800 Hz in the same manner as those for the nonspecific and specific complexes (Fig. 3*B*). (*B*) Mapping of residues that exhibited $\Delta R_2^{CPMG} > 5\ s^{-1}$ (red). Data are mapped on the crystal structure of the specific complex (PDB, 1AAY).

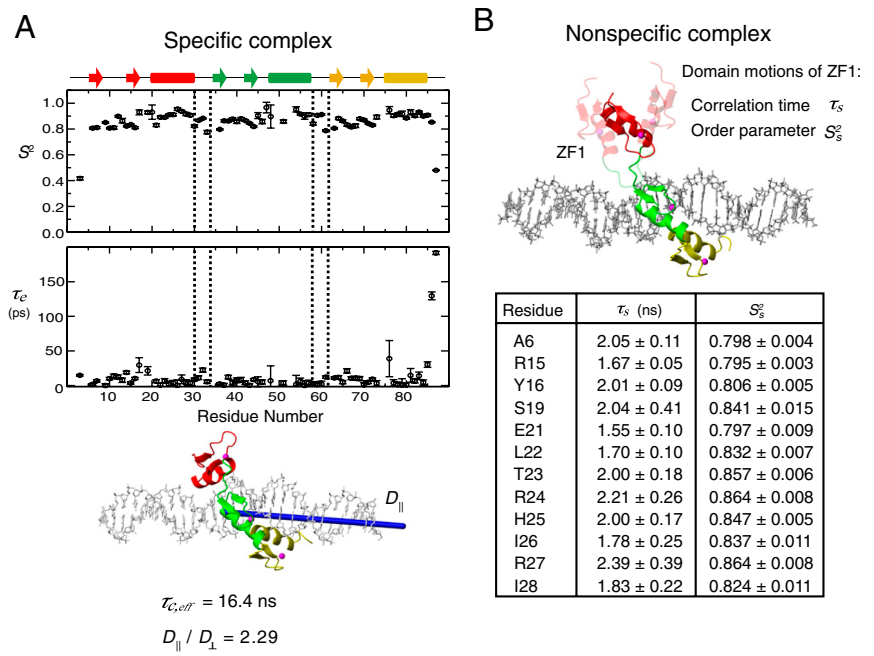


| Residue | $\tau_s$ (ns) | $S_s^2$ |
|---|---|---|
| A6 | 2.05 ± 0.11 | 0.798 ± 0.004 |
| R15 | 1.67 ± 0.05 | 0.795 ± 0.003 |
| Y16 | 2.01 ± 0.09 | 0.806 ± 0.005 |
| S19 | 2.04 ± 0.41 | 0.841 ± 0.015 |
| E21 | 1.55 ± 0.10 | 0.797 ± 0.009 |
| L22 | 1.70 ± 0.10 | 0.832 ± 0.007 |
| T23 | 2.00 ± 0.18 | 0.857 ± 0.006 |
| R24 | 2.21 ± 0.26 | 0.864 ± 0.008 |
| H25 | 2.00 ± 0.17 | 0.847 ± 0.005 |
| I26 | 1.78 ± 0.25 | 0.837 ± 0.011 |
| R27 | 2.39 ± 0.39 | 0.864 ± 0.008 |
| I28 | 1.83 ± 0.22 | 0.824 ± 0.011 |

**Fig. S3.** Additional dynamics data for the specific and nonspecific DNA complexes of Egr-1. (*A*) Order parameters and correlation times for internal motions of backbone N-H vectors in the specific DNA complex of Egr-1. These parameters were calculated using an axially symmetric diffusion model. The symmetric axis of the diffusion tensor that was determined from $^{15}$N $R_2/R_1$ ratios is shown in blue together with the structure of the specific complex (1). (*B*) Correlation times and order parameters for ZF1's domain motions in the nonspecific DNA complex of Egr-1. Only residues from β-sheet and α-helix regions were used for the calculation. Details of this calculation are given in *SI Methods*.

1 Tjandra N, Feller SE, Pastor RW, Bax A (1995) Rotational diffusion anisotropy of human ubiquitin from N-15 NMR relaxation. *J Am Chem Soc* 117:12562–12566.